Polymer Chemistry

ROYAL SOCIETY OF CHEMISTRY

COMMUNICATION

View Article Online
View Journal

Cite this: DOI: 10.1039/c9py01857c

Received 9th December 2019,
Accepted 3rd February 2020

DOI: 10.1039/c9py01857c

rsc.li/polymers

Manipulating the helix–coil transition profile of synthetic polypeptides by leveraging side-chain molecular interactions†

Ziyuan Song, ‡[a] Zhengzhong Tan,‡[a] Xuetao Zheng,[b] Zihuan Fu,[b] Ettigounder Ponnusamy[c] and Jianjun Cheng *[a,b]

Polypeptides with trigger-responsive helix–coil transition behaviours are interesting biomaterials due to their helix-specific assemblies and biomedical performances. Based on the pH-sensitive, conformationally switchable triazole polypeptides, we reported the manipulation of the helix–coil transition profile, which was determined by the combined molecular interactions of triazole and other side-chain functionalities. Specifically, the introduction of side-chain hydrophobic moieties or hydrogen bonding acceptors neutralized the helix-disrupting effect of side-chain triazoles, which altered the pH-responsive conformational transition profile of the polypeptides. These results inspired us to design new triazole polypeptides bearing dimethylamino side chains, which exhibited interesting helix–coil–helix transition behaviours as the pH decreased.

Polypeptides, as a type of protein-mimetic material, have been widely studied due to their great potential in biomedical applications.[1–6] One unique feature of polypeptide materials is their identical backbone structures as natural proteins, the peptide bonds, which enable them to form ordered secondary structures including α-helices and β-sheets.[7,8] The ordered conformation of polypeptide materials endows them with promising conformation-specific properties.[9–20] For example, cationic polypeptides adopting α-helical structures showed higher cell-penetrating ability than their non-structured, random-coil analogues, and have been used as non-viral gene delivery vectors[12,21,22] and antibacterial polymers,[23] when the side-chain structures are properly designed. Because of the helix-specific properties, the development of polypeptide materials with helix–coil transition behaviours has been explored to achieve the desired functions on-demand.[10,24–31]

Several side-chain moieties have been identified as helix or sheet disruptors or stabilizers, offering us rich tools to design conformationally switchable polypeptide materials with specific trigger-responsiveness. It has been demonstrated that hydrophobic side chains stabilize the α-helical structure,[32–34] but ionic groups[33,35,36] and polar groups[25,34,37] disrupt the α-helical conformation when placed close to the backbone. Besides charged and polar groups, hydrogen bonding (H-bonding) ligands with a specific pattern were recently demonstrated as side-chain helix disruptors.[28] The incorporation of a 1,2,3-triazole group in the side chains, for instance, rendered the polypeptide conformationally switchable, due to the pH-responsive change in the H-bonding pattern. Triazole polypeptides bearing a side-chain trimethylammonium terminus, **P0** (Fig. 1a), exhibited a coil-to-helix transition when the solution pH decreased from neutral and basic conditions to acidic conditions, which was attributed to the change in the H-bonding pattern from a binary H-bonding (BHB) pattern (*i.e.*, containing both H-bonding donors and H-bonding acceptors) to a unitary H-bonding (UHB) pattern (*i.e.*, containing only H-bonding donors or acceptors) (Fig. 1b).[28] In addition, intramolecular H-bonding interactions between side-chain nucleobases have also been reported to promote the formation of β-sheets.[38,39] However, previous studies have often focused on the effect of one specific type of side-chain molecular interaction on the polypeptide conformations. The impact of combined molecular interactions on secondary structures from multiple side-chain functionalities, which has been usually observed for natural proteins,[40] is largely unexplored.

Herein, we reported the manipulation of the helix–coil transition profile of triazole polypeptides by controlling the side-chain molecular interactions. With the incorporation of helix-stabilizing moieties or specific H-bonding ligands, the pH-responsive helix–coil transition behaviour of triazole polypeptides was altered or even eliminated (Fig. 1c). In a special case, triazole polypeptides containing side-chain tertiary amines

[a]*Department of Materials Science and Engineering, University of Illinois at Urbana–Champaign, 1304 West Green Street, Urbana, Illinois 61801, USA. E-mail: jianjunc@illinois.edu*
[b]*Department of Chemistry, University of Illinois at Urbana-Champaign, 505 South Mathews Avenue, Urbana, Illinois 61801, USA*
[c]*MilliporeSigma, 545 South Ewing, St. Louis, Missouri 63103, USA*
†Electronic supplementary information (ESI) available. See DOI: 10.1039/c9py01857c
‡These authors contributed equally.

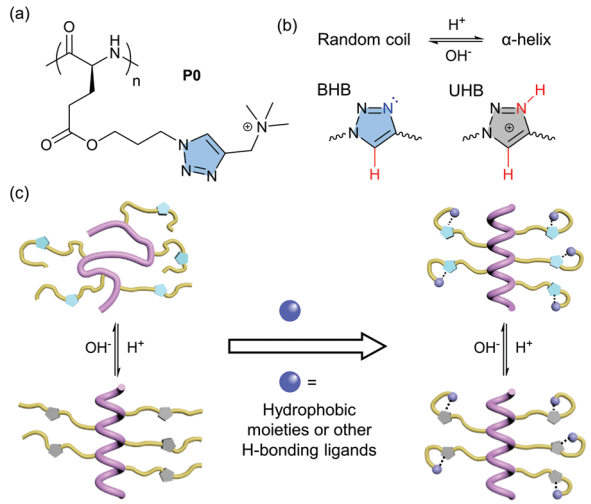

Fig. 1 (a) Chemical structure of triazole polypeptide **P0**. (b) The pH-responsive helix–coil transition of **P0** due to the change in the H-bonding pattern of side-chain triazoles. The H-bonding donors are highlighted in blue and the H-bonding acceptors are highlighted in red. (c) Scheme illustrating the change in secondary structure transition due to the incorporation of other helix-affecting moieties.

showed an interesting helix–coil–helix transition when the pH was tuned from basic to acidic conditions. We believe that this work will provide new understanding on the control over polypeptide conformations and the design of smart polypeptide materials.

Triazole polypeptides were prepared through the ring-opening polymerization (ROP) of *N*-carboxyanhydrides (NCAs), followed by post-polymerization Huisgen click chemistry (Scheme 1). Polypeptides bearing side-chain chlorines were synthesized by polymerizing γ-chloropropyl-L-glutamate NCA with *n*-hexylamine as the initiator.[13] The obtained polypeptides were characterized by gel permeation chromatography (GPC), with an obtained molecular weight M_n = 9.47 kDa and a narrow dispersity ($Đ = M_w/M_n$ = 1.18) (Fig. S1†). The side-chain chlorines were then transformed into azides, which were reacted with various alkyne molecules through copper-catalysed click reactions. The azide–alkyne click chemistry allowed the facile conjugation of a variety of functionalities with the

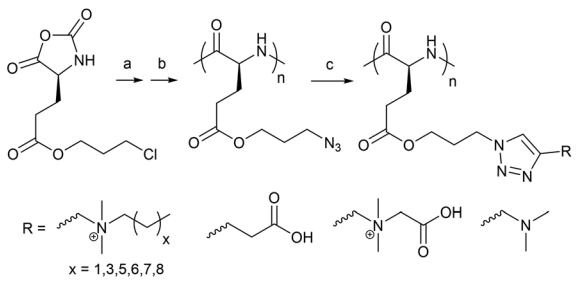

Scheme 1 Synthetic routes to triazole polypeptides *via* the polymerization of *N*-carboxyanhydrides and post-polymerization click chemistry. (a) *n*-Hexylamine, DMF, rt; (b) NaN_3, DMF, 70 °C; and (c) various alkynes, CuBr, PMDETA, DMF, rt.

natural formation of a triazole linkage, which allowed us to study the impact of these functionalities on the conformational transition behaviour of triazole polypeptides.

We first devoted our efforts in probing the impact of side-chain hydrophobic moieties, which are well known for their ability to stabilize α-helical structures.[32–34] A series of triazole polypeptides bearing ammonium side chains were synthesized, with varying lengths of alkyl substitutions to study the impact of side-chain hydrophobicity (Fig. 2a). Surprisingly, the triazole polypeptides showed good water-solubility even with an *n*-octyl ammonium substitution (*i.e.*, **P1**-Oct). Further elongating the alkyl substitutions, however, resulted in poor water-solubility which makes it difficult to study the conformation by circular dichroism (CD). As shown in Fig. 2b, triazole polypeptides **P1**-Pr and **P1**-Pe, with short hydrophobic ammonium substitutions, showed similar pH-dependent helix-to-coil transitions to those of the previously reported triazole polypeptides with a trimethyl ammonium side chain (**P0**).[28] Both polypeptides showed typical random coil CD spectra at pH 7.0, but changed to an α-helical conformation as the pH was lowered to 3.0, with double-minima CD curves being observed at 208 and 222 nm (Fig. 2b). The overlay of the CD spectra of **P1**-Pr at different pH values clearly indicated the helix–coil transition behaviour (Fig. S2†). Further increase in the alkyl length on ammonium substitution resulted in an α-helical structure for **P1**-Hex and **P1**-Hept even at pH 7.0, albeit with low helicity (19% and 20% for **P1**-Hex and **P1**-Hept,

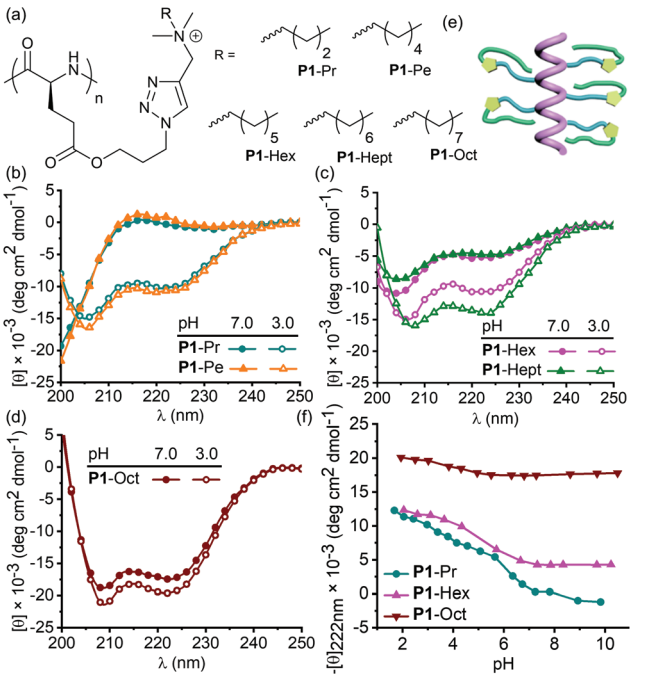

Fig. 2 (a) Chemical structures of triazole polypeptides with various hydrophobic moieties. (b–d) The CD spectra of (b) **P1**-Pr and **P1**-Pe, (c) **P1**-Hex and **P1**-Hept, and (d) **P1**-Oct at pH 7.0 and 3.0. (e) Scheme illustrating the proposed helical structure of **P1**-Oct at neutral pH. (f) pH-Ellipticity plot of **P1**-Pr, **P1**-Hex, and **P1**-Oct. The ellipticity at 222 nm was selected to indicate the helicity of the polypeptides.

respectively) (Fig. 2c). The recovery of the helical structure at neutral pH suggested that side-chain hydrophobic interactions were able to partially cancel out the disruptive effects of side-chain triazoles. The helicities of **P1**-Hex and **P1**-Hept at pH 3.0, however, remained similar to the helicities of those bearing shorter ammonium substitutions (helicity = 35% and 43% for **P1**-Hex and **P1**-Hept, respectively) (Fig. 2c). In contrast with other triazole polypeptides bearing ammonium side chains, **P1**-Oct, with an octyldimethyl ammonium side chain, exhibited strong α-helical structures at both pH = 7.0 and 3.0 with similar helicities (52% and 58% at pH 7.0 and 3.0, respectively) (Fig. 2d), demonstrating that sufficiently strong hydrophobic interactions were able to completely neutralize the side-chain helical disruptors. This result agrees well with the previous studies on ionic and polar helical disruptors.[25,33] Considering the good water-solubility and the stable helical structure of **P1**-Oct, we hypothesized that the long *n*-octyl chain folded toward the backbone (Fig. 2e and Fig. S3†), leaving the cationic charges exposed at the helical surface. Dynamic light scattering (DLS) of the aqueous solution of **P1**-Oct showed no perceptible signals, ruling out the possibility of the self-assembly of **P1**-Oct through interhelical hydrophobic interactions. The folding of the long alkyl chains greatly enhanced the side-chain hydrophobic interactions, which cancelled out the disruptive effects of triazoles. By plotting the molecular ellipticity at 222 nm against pH, we compared the pH-sensitive conformational changes of **P1**-Pr, **P1**-Hex, and **P1**-Oct (Fig. 2f). It is the competition between the stabilizing effect from hydrophobic moieties and the disruptive effect from triazoles that determined the helix–coil transition profiles of triazole polypeptides with various ammonium substitutions. **P1**-Pr exhibited a gradual change in conformation over a broad pH range, likely due to the broad buffering effect of side-chain triazoles.[28] The increase in the alkyl lengths of ammonium substitution strengthened the side-chain hydrophobic interactions, resulting in the recovery of helices at pH 7–10. With sufficiently strong side-chain hydrophobicity, a pH-independent conformation was observed for **P1**-Oct, with complete elimination of the helix–coil transition behaviour.

In an attempt to investigate the impacts of the charge type, we synthesized triazole polypeptides bearing a side-chain carboxylic acid (**P2**-CA) (Fig. 3a). **P2**-CA adopted an unexpected α-helical structure with a strong helicity of 40% at pH 7.0, with further increase in the helicity to 62% at pH 5.0 (Fig. 3b). A further decrease in aqueous pH resulted in the precipitation of polypeptides from solution, likely due to the protonation of side-chain carboxylic acids, in a similar way to that of poly(L-glutamatic acid).[36,41] Since carboxylic acids can also serve as H-bonding acceptors,[42] we reasoned that the recovery of the helical structure of **P2**-CA at pH 7.0 may result from the change in the H-bonding pattern of triazoles. The H-bonding interactions between side-chain carboxylic acids and triazoles saturated the H-bonding donor on the triazole ring, switching the triazole from a BHB pattern to a "pseudo-UHB" pattern with decreased disruptive effects on backbone helices (Fig. 3c). In order to validate our hypothesis on the pseudo-UHB pattern, a

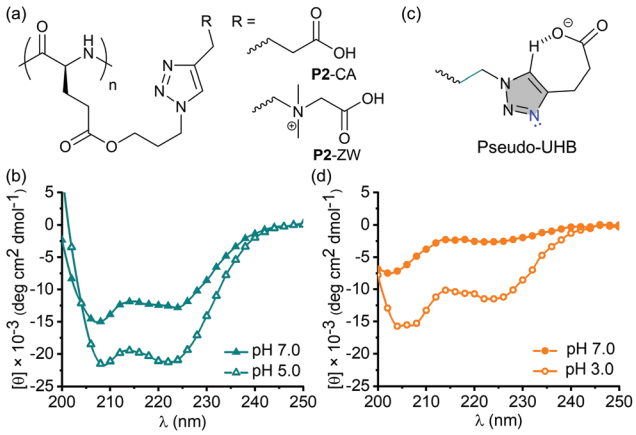

Fig. 3 (a) Chemical structures of polypeptides **P2**-CA and **P2**-ZW. (b) The CD spectra of **P2**-CA at pH 7.0 and 5.0. (c) The H-bonding pattern of the side chains of **P2**-CA changed to pseudo-UHB under neutral conditions. (d) The CD spectra of **P2**-ZW at pH 7.0 and 3.0.

zwitterionic triazole polypeptide, **P2**-ZW, was synthesized as an analogue of **P0** bearing H-bonding acceptors (Fig. 3a). Recovery of helicity was also observed for **P2**-ZW at pH 7.0 (Fig. 3d), ruling out the possibility that the elimination of the coiled conformation of **P2**-CA resulted from the removal of the ammonium units. **P2**-ZW exhibited a lower helicity than **P2**-CA at pH 7.0, likely due to the weaker H-bonding interactions between carboxylic acids and triazoles (an 8-membered ring with a cationic charge for **P2**-ZW, compared with a 7-membered ring for **P2**-CA). The strength of H-bonding was dependent on not only the intramolecular H-bonding ring size, but also the type of H-bonding receptors and other parameters.[43,44] Therefore, a more detailed analysis is currently underway, which will further reveal the relationship between the side-chain H-bonding strength and the disrupting ability of triazoles. Nevertheless, the side-chain H-bonding interactions only partially deactivate the triazole disruptors, as increased helicity was still observed for both **P2**-CA and **P2**-ZW, due to the protonation of triazole into triazolium at acidic pH (Fig. 3b, d, and Fig. S4†).

The conformation of **P2**-CA and **P2**-ZW inspired us to design polypeptides with new helix–coil transition profiles. We incorporated dimethylamino groups, which exhibited pH-responsive H-bonding patterns, into the side chains of triazole polypeptides **P3** (Fig. 4a). The side-chain tertiary amine serves as a H-bonding acceptor under basic conditions, but loses its H-bonding accepting ability when protonated (Fig. 4b). Under basic conditions (pH > 7), **P3** adopted a stable α-helical structure with a helicity of ~42% (Fig. 4c), where the side-chain triazole was deactivated into a pseudo-UHB ligand, similar to that of **P2**-CA, due to the H-bonding interactions with the side-chain tertiary amine. The decrease in aqueous pH led to the protonation of tertiary amines, causing a decrease in the helicity (helicity ~ 19%) as the pH dropped to 4.0 (Fig. 4d). The protonation of tertiary amines activated the side-chain triazoles (BHB pattern), resulting in the disruption of the α-helical conformation. Further acidification of the aqueous

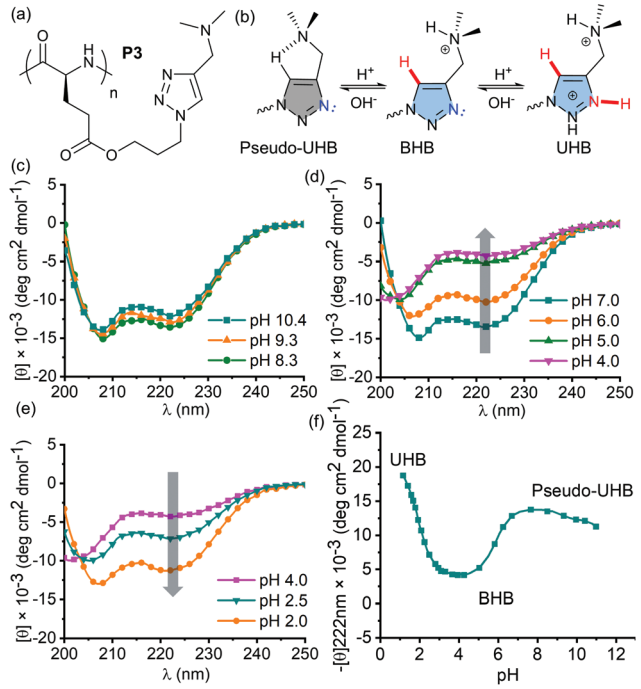

Fig. 4 (a) Chemical structures of polypeptides **P3**. (b) The change in the side-chain H-bonding pattern with pH. (c–e) CD spectra of **P3** in the pH range of (c) 8.0–10.5, (d) 4.0–7.0, and (e) 2.0–4.0. (d) pH-Ellipticity plot of **P3**. The ellipticity at 222 nm was selected to indicate the helicity of polypeptides.

solution led to the recovery of the helical structure with an enhanced helicity (helicity 37% at pH 2.0), which was attributed to the protonation of triazoles (Fig. 4e). Therefore, we were able to control the secondary structure of **P3** by manipulating the interactions between side-chain tertiary amines and side-chain triazoles. The change in the H-bonding pattern of polypeptide side chains from pseudo-UHB to BHB and UHB, with a decrease in aqueous pH, resulted in the helix–coil–helix transition profile of **P3** (Fig. 4f).

In summary, we have shown the manipulation of the helix–coil transition profile of synthetic polypeptides using various molecular interactions with incorporated side-chain functionalities. The use of combined interactions enhanced the magnitude of complexity of structure control, which played a crucial role in determining the conformation of polypeptides. We believe that this study will pave the way for the future development of smart synthetic polymers that exhibit conformation-specific functions under the desired conditions.

Conflicts of interest

There are no conflicts to declare.

Acknowledgements

This work was supported by the National Science Foundation (CHE-1709820).

Notes and references

1 T. J. Deming, *Prog. Polym. Sci.*, 2007, **32**, 858–875.
2 K. Kataoka, A. Harada and Y. Nagasaki, *Adv. Drug Delivery Rev.*, 2012, **64**, 37–48.
3 C. Deng, J. Wu, R. Cheng, F. Meng, H.-A. Klok and Z. Zhong, *Prog. Polym. Sci.*, 2014, **39**, 330–364.
4 H. Lu, J. Wang, Z. Song, L. Yin, Y. Zhang, H. Tang, C. Tu, Y. Lin and J. Cheng, *Chem. Commun.*, 2014, **50**, 139–155.
5 Z. Song, Z. Han, S. Lv, C. Chen, L. Chen, L. Yin and J. Cheng, *Chem. Soc. Rev.*, 2017, **46**, 6570–6599.
6 Z. Song, Z. Tan and J. Cheng, *Macromolecules*, 2019, **52**, 8521–8539.
7 C. Bonduelle, *Polym. Chem.*, 2018, **9**, 1517–1529.
8 Z. Song, H. Fu, R. Wang, L. A. Pacheco, X. Wang, Y. Lin and J. Cheng, *Chem. Soc. Rev.*, 2018, **47**, 7401–7425.
9 A. P. Nowak, V. Breedveld, L. Pakstis, B. Ozbas, D. J. Pine, D. Pochan and T. J. Deming, *Nature*, 2002, **417**, 424–428.
10 E. G. Bellomo, M. D. Wyrsta, L. Pakstis, D. J. Pochan and T. J. Deming, *Nat. Mater.*, 2004, **3**, 244–248.
11 K. Osada, H. Cabral, Y. Mochida, S. Lee, K. Nagata, T. Matsuura, M. Yamamoto, Y. Anraku, A. Kishimura, N. Nishiyama and K. Kataoka, *J. Am. Chem. Soc.*, 2012, **134**, 13172–13175.
12 N. P. Gabrielson, H. Lu, L. Yin, D. Li, F. Wang and J. Cheng, *Angew. Chem., Int. Ed.*, 2012, **51**, 1143–1147.
13 H. Tang, L. Yin, K. H. Kim and J. Cheng, *Chem. Sci.*, 2013, **4**, 3839–3844.
14 Y. Mochida, H. Cabral, Y. Miura, F. Albertini, S. Fukushima, K. Osada, N. Nishiyama and K. Kataoka, *ACS Nano*, 2014, **8**, 6724–6738.
15 S. L. Perry, L. Leon, K. Q. Hoffmann, M. J. Kade, D. Priftis, K. A. Black, D. Wong, R. A. Klein, C. F. Pierce, K. O. Margossian, J. K. Whitmer, J. Qin, J. J. de Pablo and M. Tirrell, *Nat. Commun.*, 2015, **6**, 6052.
16 R. Baumgartner, H. Fu, Z. Song, Y. Lin and J. Cheng, *Nat. Chem.*, 2017, **9**, 614–622.
17 T. Kaneko, M. A. Ali, I. Captain, P. Perlin and T. J. Deming, *Polym. Chem.*, 2018, **9**, 3466–3472.
18 J. Aujard-Catot, M. Nguyen, C. Bijani, G. Pratviel and C. Bonduelle, *Polym. Chem.*, 2018, **9**, 4100–4107.
19 Y. Hou, Y. Zhou, H. Wang, J. Sun, R. Wang, K. Sheng, J. Yuan, Y. Hu, Y. Chao, Z. Liu and H. Lu, *ACS Cent. Sci.*, 2019, **5**, 229–236.
20 Z. Song, H. Fu, R. Baumgartner, L. Zhu, K.-C. Shih, Y. Xia, X. Zheng, L. Yin, C. Chipot, Y. Lin and J. Cheng, *Nat. Commun.*, 2019, **10**, 5470.
21 L. Yin, Z. Song, K. H. Kim, N. Zheng, N. P. Gabrielson and J. Cheng, *Adv. Mater.*, 2013, **25**, 3063–3070.
22 L. Yin, Z. Song, Q. Qu, K. H. Kim, N. Zheng, C. Yao, I. Chaudhury, H. Tang, N. P. Gabrielson, F. M. Uckun and J. Cheng, *Angew. Chem., Int. Ed.*, 2013, **52**, 5757–5761.
23 M. Xiong, Y. Bao, X. Xu, H. Wang, Z. Han, Z. Wang, Y. Liu, S. Huang, Z. Song, J. Chen, R. M. Peek Jr., L. Yin, L. F. Chen and J. Cheng, *Proc. Natl. Acad. Sci. U. S. A.*, 2017, **114**, 12675–12680.

24 J. Rodriguez-Hernandez and S. Lecommandoux, *J. Am. Chem. Soc.*, 2005, **127**, 2026–2027.
25 J. R. Kramer and T. J. Deming, *J. Am. Chem. Soc.*, 2012, **134**, 4112–4115.
26 A. R. Rodriguez, J. R. Kramer and T. J. Deming, *Biomacromolecules*, 2013, **14**, 3610–3614.
27 L. Yin, H. Tang, K. H. Kim, N. Zheng, Z. Song, N. P. Gabrielson, H. Lu and J. Cheng, *Angew. Chem., Int. Ed.*, 2013, **52**, 9182–9186.
28 Z. Song, R. A. Mansbach, H. He, K. C. Shih, R. Baumgartner, N. Zheng, X. Ba, Y. Huang, D. Mani, Y. Liu, Y. Lin, M. P. Nieh, A. L. Ferguson, L. Yin and J. Cheng, *Nat. Commun.*, 2017, **8**, 92.
29 M. Xiong, Z. Han, Z. Song, J. Yu, H. Ying, L. Yin and J. Cheng, *Angew. Chem., Int. Ed.*, 2017, **56**, 10826–10829.
30 H. Xia, H. Fu, Y. Zhang, K.-C. Shih, Y. Ren, M. Anuganti, M.-P. Nieh, J. Cheng and Y. Lin, *J. Am. Chem. Soc.*, 2017, **139**, 11106–11116.
31 J. Yuan, Y. Zhang, Y. Sun, Z. Cai, L. Yang and H. Lu, *Biomacromolecules*, 2018, **19**, 2089–2097.
32 N. Lotan, A. Yaron and A. Berger, *Biopolymers*, 1966, **4**, 365–368.
33 H. Lu, J. Wang, Y. Bai, J. W. Lang, S. Liu, Y. Lin and J. Cheng, *Nat. Commun.*, 2011, **2**, 206.
34 E. G. Gharakhanian, E. Bahrun and T. J. Deming, *J. Am. Chem. Soc.*, 2019, **141**, 14530–14533.
35 E. R. Blout and M. Idelson, *J. Am. Chem. Soc.*, 1956, **78**, 497–498.
36 P. Doty, A. Wada, J. T. Yang and E. R. Blout, *J. Polym. Sci.*, 1957, **23**, 851–861.
37 H. Liu, R. Wang, J. Wei, C. Cheng, Y. Zheng, Y. Pan, X. He, M. Ding, H. Tan and Q. Fu, *J. Am. Chem. Soc.*, 2018, **140**, 6604–6610.
38 M. Nguyen, J.-L. Stigliani, G. Pratviel and C. Bonduelle, *Chem. Commun.*, 2017, **53**, 7501–7504.
39 M. Nguyen, J.-L. Stigliani, C. Bijani, P. Verhaeghe, G. Pratviel and C. Bonduelle, *Biomacromolecules*, 2018, **19**, 4068–4074.
40 P. A. Frey, S. A. Whitt and J. B. Tobin, *Science*, 1994, **264**, 1927–1930.
41 K. S. Krannig and H. Schlaad, *J. Am. Chem. Soc.*, 2012, **134**, 18542–18545.
42 M. C. Etter, *J. Am. Chem. Soc.*, 1982, **104**, 1095–1096.
43 J. J. Novoa and M. H. Whangbo, *J. Am. Chem. Soc.*, 1991, **113**, 9017–9026.
44 S. Wojtulewski and S. J. Grabowski, *Chem. Phys. Lett.*, 2003, **378**, 388–394.